3-13-2006

Rotational and Cyclical Variability in γ Cassiopeia

Myron A. Smith
The Catholic University of America

Gregory W. Henry
Tennessee State University

Ethan Vishniac
Johns Hopkins University

Version of July 3, 2018

Rotational and Cyclical Variability in γ Cas

Myron A. Smith,

Catholic University of America,
3700 San Martin Dr., Baltimore, MD 21218;
msmith@stsci.edu,

Gregory W. Henry

Center of Excellence in Information Systems,
Tennessee State University,
3500 John A. Merritt Blvd., Nashville, TN 37209;
henry@schwab.tsuniv.edu,

and

Ethan Vishniac

Department of Physics and Astronomy,
The Johns Hopkins University,
3400 N. Charles St.,
Baltimore, MD 21218;
ethan@pha.jhu.edu

ABSTRACT

γ Cas is an unusual classical Be star for which the optical-band and hard X-ray fluxes vary on a variety of timescales. We report results of a nine-year monitoring effort on this star with a robotic ground-based (APT) telescope in the B, V filter system as well as simultaneous observations in 2004 November with this instrument and the *Rossi X-ray Timing Explorer (RXTE)* telescope. Our observations disclosed no correlated optical response to the rapid X-ray flares in this star, nor did the star show any sustained flux changes any time during two monitored nights in either wavelength regime. Optical light curves obtained in the APT program revealed, consistent with an earlier study by Robinson et al., that γ Cas undergoes $\sim$3%-amplitude cycles with lengths of 60–90 days. Our observations in 2004 showed a similar optical cycle. Over the nine days

we monitored the star with the *RXTE*, the X-ray flux varied in phase with its optical cycle and with an amplitude predicted from the data in Robinson et al. In general, the amplitude of the V magnitude cycles are 30–40% larger than the corresponding B amplitude, suggesting the seat of the cycles is circumstellar. The cycle lengths constantly change and can damp or grow on timescales as short as 13 days. We have also discovered a coherent period of 1.21581±0.00002 days in all our data, which is consistent only with rotation. The full amplitude of this variation is 0.0060 in both filters, and surprisingly, its waveform is almost sawtooth in shape. This variation probably originates on the star's surface. This circumstance hints at the existence of a strong magnetic field with a complex topology and an associated heterogeneous surface composition.

Subject headings: :

stars: individual (γ Cas) – stars: emission-line, Be – optical: stars – X-rays: stars

1. Introduction

Discovered as the first of its class in 1867, γ Cas (B0.5 IV) is by definition the prototype of "classical Be stars."[1] Its strong Hα emission arises from a disk that is among a handful that has been observed in the infrared, millimeter, and centimeter radio regions. Its emission is due in large part to the disk's high central density of 10^{13} cm^{-3}, which is among the highest known for classical Be stars (e.g., Waters, Coté, and Lamers 1987). The disk has been imaged interferometrically in Hα flux by several groups (e.g., Quirrenbach et al. 1996, Tycner et al. 2004) out to a distance of at least 6R$_*$. Measurements of the semiminor to semimajor axis ratio of this image permit estimates of the rotational inclination of the star/disk rotational axis: $i = 46^o$ and 60^o, respectively. Berio et al. (1999) have imaged a dense azimuthal sector of the disk which orbited the star with a period of several years. This structure is likely due to a one-armed density pattern that develop in perhaps $\frac{1}{4}$ of all Be stars (Hummel 2000) and are responsible for the oscillating ratio of the V and R Hα emission components in many of these stars. The effect of the star's radiative wind and stellar disk on its immediate environment is yet to be determined. Recently, Harmanec et al. (2000) and Miroschnichenko et al. (2002) have found that γ Cas is in a 204-day binary with a low eccentricity. The evolutionary status of the low-mass secondary is unknown. Given the orbital separation of this system, it is possible that the gravitational perturbations from the secondary are important in truncating the outer edge of the disk (Okazaki & Negueruela 2001).

Although γ Cas is typical for a Be star in most of these respects, it is highly unusual in others. Chief among its peculiarities is a rich array of variability patterns in the optical, ultraviolet, and X-ray regimes which extend from timescales of seconds to years (e.g., Horaguchi et al. 1994, Harmanec 2002). A proper understanding the interrelationship between these variabilities requires a series of dedicated time sequences of observations in both wavelength domains. This paper represents a continuation of a series of efforts dedicated to determining how these various patterns are related using simultaneous or contemporaneous satellites, including the *Goddard High Resolution Spectrograph* (GHRS) attached to the *Hubble Space Telescope (HST)*, the Rossi X-ray Timing Explorer (RXTE) and the *International Ultraviolet Explorer (IUE).*

The coordinated X-ray prong of this campaign consisted of a simultaneous 22 hour monitoring in January of 1996 with the *GHRS* and *RXTE.* A quasi-continuum light curve generated from the *GHRS* spectra exhibited a pair of 1–2% dips over a few hours. The si-

[1]We define classical Be star succinctly as a single, post-ZAMS Be star which has somehow expelled matter which has settled into a disk confined to the rotational plane.

multaneous *RXTE* fluxes showed maxima at these same times (Smith, Robinson, & Corbet 1998). Subsequent analysis showed that the ultraviolet dips cannot arise on the Be star's surface and are most likely to occur from co-rotating "clouds" close to the star's surface (Smith, Robinson, & Hatzes 1998, hereafter SRH98). The same ultraviolet spectra showed many sharp features similar to the long known blue-to-red "migrating subfeatures" in the star's optical line profiles (Yang, Ninkov, & Walker 1988, Smith 1995, Smith & Robinson 1998). A central conclusion of this program was that the immediate circumstellar environment of γ Cas, even beyond the equatorial plane, is highly complex. The system of corotating clouds (some heated and some cooled; Smith & Robinson 2000) alone constitutes a more complex environments than is indicated for most, if not all, other Be stars. Moreover, the clouds require a mechanism to anchor them onto fixed points on the surface. Such a mechanism may be presumed to be a strong magnetic field, but the discovery of a postulated field in this rapidly rotating star seems beyond the reach of present spectropolarimetric detection devices. This fact suggests that one must search for indirect indicators of magnetic field that can test this picture.

Accordingly, in 1997 Robinson, Smith, & Henry (2002, hereafter RSH02) mounted a long-term robotic photometric monitoring campaign on this star in the Johnson B and V system using an Automated Photometric Telescope (APT) in Arizona. Our program was to search for optical signatures of activity unique to γ Cas and especially those correlated with known X-ray activity over a range of timescales. These included the rotational timescale, estimated to be near one day, as well as longer-term variations that he *RXTE* campaigns and earlier observations on other X-ray satellites had suggested are present. Soon after they initiated this program, RSH02 identified a strong pattern characterized as small-amplitude, long (60–90 days) cycles. The fluxes from 8 *RXTE* observations matched these cycles in length and phase but with amplitudes of nearly 100 times larger. Because the energy associated with the optical variations is much larger than in the X-ray variations, this correlation cannot be interpreted simply as a reprocessing of the X-ray modulation, and one must seek another explanation. One clue to this interpretation is that the optical variations have a color consistent with the brightening/color trajectories that accompany the evolution of the disks of γ Cas and other Be stars. This fact suggests that the optical variations arise in the disk. Based on both the cyclicity and redness of the optical variations, RSH02 conjectured that both the optical variations and the generation of anomalous X-rays in γ Cas was produced by a Balbus-Hawley instability leading to a disk dynamo. Furthermore, the winding up of putative field lines from the star with the interaction of the keplerian disk would and stretch and sever their connection. The ensuing reconnection would accelerate disk atoms in the form of high energy beams, which would generate X-rays when they impacted the surface of the Be star. The observation of absorption systems redshifted to 2,000 $\mathrm{km\,s^{-1}}$ in

the *GHRS* spectra (Smith & Robinson 2000) is consistent with the geometric and kinematic requirements of this speculative picture.

This paper presents the results of searches for rapid- and intermediate-timescale correlations of optical and X-ray fluxes of γ Cas. In §4 we describe newly found characteristics of the long-term cycles found by RSH02 from 9 seasons of optical robotic data. In §5 we report the results of a successful search from this dataset for a periodicity consistent with the star's expected rotational period and discuss its implications for models of this star's X-ray emission.

2. Observations

2.1. Optical data

The optical photometry discussed in this paper was acquired with the T3 0.4-meter Automated Photometric Telescope (APT) located at Fairborn Observatory in southern Arizona. The photometer uses a temperature-stabilized EMI 9924B photomultiplier tube to acquire data successively in the Johnson B and V filter passbands. The observations of γ Cas were acquired in the following sequence, termed a group observation: *K, sky, C, V, C, V, C, V, C, sky, K*, where K is the check star HD 5395 ($V = 4.62$, $B - V = 0.96$, G8IIIb), C is the comparison star HD 6210 ($V = 5.83$, $B - V = 0.57$, F6 V), and V is the program star γ Cas ($V = 2.15$, $B - V = -0.05$, B0.5 IV). To avoid saturating the photomultiplier tube when observing γ Cas, we made the observations through a 3.8 magnitude neutral density filter. We used 10 second integration times for γ Cas and HD 5395 and 20 seconds for HD 6210 and the sky readings.

Three variable-minus-comparison and two check-minus-comparison differential magnitudes in each photometric band were computed for each group observation and then averaged to create group-mean differential magnitudes. The group means were corrected for differential extinction with nightly extinction coefficients, transformed to the Johnson system with yearly mean transformation coefficients, and treated as single observations thereafter. Typically, several group observations were made each clear night at intervals of approximately two hours. The external precision of the group means, based on standard deviations for pairs of constant stars, is typically ± 0.004 magnitudes However, point-to-point observations on intensively monitored nights were found to have a mean deviation of only ± 0.003 mag. Group means with a standard deviation greater than 0.01 mag were discarded. Further details of telescope operations and data-reduction procedures can be found in Henry (1995a,b).

Our photometric γ Cas observing program began in 1997 September and at this writ-

ing is still continuing. Our cutoff date for reporting data in this paper is 2006 February. Typically we succeeded in obtaining a few nights of data at the beginning of each observing season in June before the Arizona rainy season forced us to close the APT operations for the summer beginning around 4 July each year. We resumed the monitoring of γ Cas in mid-September each year and continued through the end of each observing season in February. Our observations during the first observing season between 1997 September and 1998 February (JD 2450718 through 2450856) were made using different neutral density filters for γ Cas and the other stars in the group. We found it difficult to calibrate the final reduced magnitudes properly. Therefore, these first-season observations have an undetermined offset with respect to observations in the rest of the seasons. The instrumental setup was stable for observing seasons two (1998/1999) through nine (2005/2006). Our dataset over 9 seasons includes 3157 B and 3135 V observations. A sample of our differential magnitudes is tabulated in Table 1. The full dataset is available in the on-line version of this paper. (Entries of "99.999" are placeholders when only a partial observation was obtained due to interference by possible faint clouds.) For plotting purposes, we added to our differential magnitudes the apparent V and B magnitudes of the comparison star ($m_V = 5.84$, $m_B = 6.40$, respectively; after Breger 1974) to establish the proper zeropoint for our measures of γ Cas.

Beginning in the 2000/2001 season, we made an effort dedicate occasional full nights ($\approx$8 hours) to the γ Cas program. A major effort to observe this star simultaneously with the *RXTE* satellite consisted of our attempting to observe intensively during the nights just preceding and following four coordinated nights in 2004 November, as well as the nights themselves. Altogether, 13 nights of the sustained monitorings are included in our dataset, as sell as several other nights of 5 hours or longer. The cadence rate of these intensive observations was one group cycle every 8 to 4 minutes.

2.2. *RXTE* Data

The X-ray component of our program consisted of monitoring γ Cas with the *Rossi X-ray Timing Explorer* (*RXTE*) satellite using the Proportional Counter Array (PCA), which detects photons in the 2–30 keV energy range. We used the FTOOLS reduction package to complete the pipeline processing of the data and to generate "Standard 2" light curves with a bin time of 16 seconds.

This program, designated P90001 in the Guest Observer Cycle 9, was designed to monitor this star at the same times our APT system was active during nighttime in Arizona. As a hedge against inclement weather, we asked the *RXTE* project to monitor the satellite during 4 orbits on each of four nights distributed over several days during a time when γ Cas

was situated close to the Continuous Viewing Zone of the satellite. The project was able to meet this request by allocating 8 hours on each of the nights of 2004 November 5, 9, 13, and 14 (UT dates). Our results met the statistics we expected (i.e., they were neither lucky nor unlucky) since it turned out that we obtained overlap with the APT monitoring on 2 of the 4 nights. Counting brief interruptions from Earth occultation, SAA passages, and a high radiation storm, we obtained a total on-target time of 21.3 hours on γ Cas.

During nearly all the PCA observations, three of the five PCU detectors actively integrated on our target. All count rates represented in §3 are scaled by 5/3 to make them directly comparable with the rates given by Smith, Robinson, & Corbet (1998, hereafter SRC98). The *RXTE*/PCA is an efficient photon detecting system, and the errors in the net light curve are elevated by only several percent above the combined Poisson errors of the gross and model background fluxes (see also SRC98).

3. Rapid Optical and X-ray Variability

3.1. Optical Color Variations

The first step in our analysis of the optical APT data was to determine the mean $\Delta B/\Delta V$ slopes of the variations, which RSH02 showed to be dominated by the optical cycles. We plotted the V against B magnitudes for each of the 9 seasons and found that the mean color slope is 0.69. However, we found that these slope values seem to cluster around two values of about 0.63 and 0.73. For example, there are no season-averaged slopes in the range 0.66–0.70. Since the formal significance of each of the seasonal average ratios, including the observational errors is about ± 0.05, these differences are marginally statistically significant to 3σ for the two seasonal group means. We show an example of these contrasting behaviors for seasons 2000/2001 ("2000") and 2001/2002 in Figure 1. Inspection of this plot discloses that the 2001/2002 magnitudes (squares) have a steeper slope than the 2000/2001 data (dots). The respective slopes for these two seasons are 0.73 and 0.61.

The reddish color implied by these ratios implies that the cyclical flux changes originate in gas cooler than the effective temperature of the Be star. Following RSH02, we suggest that this region is part of the star's decretion disk for two reasons. First, extensive Be disks are well known to contribute to the color of a Be star. No other structure (or star) exists near γ Cas that could be responsible for a 2–3% variation in the combined optical light. Second, this change is consistent with the color changes observed during the evolution of disks, both in other Be stars and γ Cas itself. If continued accumulation of seasonal averages supports this implied bimodality (4 low values, 5 high), it would likely mean that the variations are

caused in different spatial regions of the disk. However, this speculation will take at least a few more years of monitoring to substantiate.

3.2. Rapid X-ray/optical variations

Our attempt to obtain comparisons of simultaneous observations of light and X-ray flux variability was significantly marred by ground or satellite "weather" during each of our four nights of observations in 2004 November. On November 5, we obtained *RXTE* data during a total span of 3 hours, but about $\frac{1}{2}$ of this collection was interrupted by the detectors' shutting off during the *RXTE* satellite's passage through the SAA or cloudy weather in Arizona. Our most successful monitoring lasted 7.2 hours on the night of November 9, though it was interrupted by a 2-hour radiation storm. On November 13 the target was monitored over 1.7 hours, of which about 0.6 hours was interrupted by a SAA passage. No APT data were collected due to cloudy weather on November 14. To compare the first three nights of X-ray and optical fluxes, we binned the *RXTE* 16-second data to the APT's time sampling of about 10 minutes and compared these means with any APT observations within 8 minutes of each mean. This gave 4, 24, and 10 paired simultaneous observations for November 5, 9, and 13, respectively. The data for November 5 were insufficient for comparison.

In Figure 2 we depict the simultaneous APT and *RXTE* for γ Cas on November 9th. Because the mean was not well determined, we disregarded the data from November 5 and examined the deviations of the X-ray and optical fluxes from their nightly mean values. As the reader might suspect from visual inspection of Fig. 2, the deviations of the X-ray and APT data show no trend at all.[2] Indeed, the correlation coefficients in the X-ray/optical fluctuation scatter diagrams are less than ± 0.1, and these values are changed insignificantly when regressions are run including the effects of errors in the observations. In any case, if we adopt the ratio of X-ray/optical flux variations from RSH02 and 1997–2004 seasons in §4 below, namely $\Delta \mathrm{L}_x/\Delta V = 3.0/.0366 \approx 80 \pm 20$, we find that our scatter plots from November 9 are significantly different from this relation by 8σ and 12σ for the B and V filters. The same statement can be made to a significance level of 7σ for the November 13 data. The absence of an optical/X-ray correlation on a rapid (tens of minutes to a few hours) is consistent with the results of SRC98, who found no response in the UV continuum light curve of 1996 March 15 while at the same time *RXTE* observed almost continuous X-ray flaring.

[2]We obtained the same null result when we shifted the X-ray fluxes in time by up to ± 14 minutes to account for the contingency that this flux comes from the secondary of the γ Cas system.

3.3. Intermediate timescale optical/X-ray variations

3.3.1. Monotonic trends in optical data over several hours

In inspecting the nights of intensive APT monitoring, we found that ≃1% variations with timescales of up to eight hours are common. Two of these V and B variations, consisting of rapid light dips or increases, were discussed in RSH02 (see their Fig. 10) and were a motivation for the present study. However, we also found times for which the optical light brightened or dimmed monotonically during an entire 8-hour night. Figure 3 exhibits the V and B magnitude time series for the nights of 2003 November 19 and 20. For both nights and in both filters the optical light level rises or falls over the course of ≈8 hours. The significances of these trends are 6.2σ and 4.6σ (V filter) and 5.3σ and 3.7σ (B-filter).

It is of interest to examine archival X-ray light curves of γ Cas to see whether they exhibit a similar behavior. In particular, we ask what X-ray changes would be implied by these trends if they followed the X-ray/optical correlated flux ratio of ∼80? For the data in Fig. 3, the optical trends would then translate to X-ray variations of about 50%. To answer the question of whether the X-ray fluxes show a similar behavior, one can consult the homogeneous *RXTE* light curves published in Figure 6 of RSH02. These data represent the results of six 27-hour monitorings of this star with this instrument during 2000. The light curves show that over 8 hour stretches one can find five similarly sustained changes in the X-ray flux having full amplitudes of 50% or more. These include three increases during Visits 1, 2, and 5 of these monitorings and two decreases during Visits 2 and 5. These variations comprise 5 "events" in 112 hours of *RXTE* observation, or one every 22.4 hours.

To compare the frequency of optical and *RXTE* events, we examined the light curves of 13 nights during which the APT monitored γ Cas intensively (37–59 observations) in each bandpass. On these nights we found five nights of sustained increases of about ≃0.01 mags. (on HJD - 2450000 = 52230, 52962, 53283, 53319–20), two nights of decreases (51866 and 52215), and six nights of negligible net change (51831, 51834, 52966–7, 53318, and 53322). In all cases these trends were significant to at least 3σ, and the V and B filter data showed the same trends or constancy. Altogether, the history from the intensive APT observations show seven up/down trends in 104 hours, or an optical rate of one trend event per 14.9±5 hours of monitoring. This is comparable to the X-ray rate of one event per 22.4±10 hours. All told, on any given night the probability of observing a trend is ∼7/13. We were apparently unlucky not to catch one of these events in any our four planned all-night monitorings. In any case, it is *plausible,* based on these statistical arguments that the two behaviors are related to one another, and that the $\Delta B/\Delta V$ ratio during a night's observations is close to the ratio found in the correlated long-term cycles. The rhetorical question before us is whether

statistical arguments alone based on nonsimultaneous events are a compelling argument for an X-ray/optical correlation.

3.3.2. How can the intermediate-term X-ray and optical variations be understood?

Clearly, the above question must be answered in the negative because frequency arguments based on the present data are insufficient to demonstrate that the X-ray and optical variations are correlated. However, if this is not the case, one has the problem of explaining how two new phenomena are produced. The optical variations, which likewise have a $\Delta V/\Delta B$ ratio of $1.20\pm.07$ (e.g., Fig. 3), are difficult to understand in their own right. The implied color term suggests that they are formed in a cool (circumstellar) environment. That they are visible at all implies that they are likely to be formed over volumes considerably larger than the UV-absorbing corotating "clouds" of size 0.2–0.3R_*. This logic implies that they are most likely to arise in short-lived dense volumes within the disk. If future observations continue to imply that X-ray and optical trend-events occur together with mutually consistent slopes, it may be possible to identify them with local cells that occasionally break away from a generally organized global oscillation of the disk. This would explain why these variations adhere to the X-ray/optical ratio of 80. We note that such occurrences are actually common in astrophysical dynamos, for example manifesting themselves as "stray" sunspots that appear "out of phase" during solar cycles.

4. The Long-term Cycles

4.1. Continued correlation of X-ray and optical cycles

A key result of the RSH02 study was the discovery of a correlation between optical and X-ray cycles of roughly 70 days. This correlation was made possible by a total of eight 27-hour *RXTE* observations that were contemporaneous with the APT observations in 1998 and 2000. In this paper we report on *RXTE* observations that span a total of nine days. Although this is a much shorter time than a cycle length, the phasing of the new *RXTE* data near the maximum of the optical cycle allow one to predict an X-ray flux at the peak of its cycle and to compare it with the observations. Moreover, our range of nine days over which the *RXTE* observations were made in 2004 November is large enough to compare with the *slope* of the predicted X-ray variation inferred from the ephemeris for the optical cycle during the 2004/5 season, as discussed in the next section. The maximum for the sinusoid is taken from X-ray flux maximum (90 cts s^{-1}) that correspond to the optical maximum,

according to RSH02. Fig. 4 exhibits this comparison. The dots represent the individual X-ray observations. The scatter in these data are mainly fluctuations in the X-ray fluxes caused by flares and changes in the basal flux contribution. The dashed line in this figure is the RSH02 prediction for the maximum of an optical cycle. We emphasize that other than applying the X-ray/optical conversion factor of 80, *no scaling or adjustments have been made in constructing the sinusoidal curve in this figure.* The agreement of the trend represented by the dashed curve to the data represents a confirmation of the correlation of the X-ray and optical cycles found by RSH02.

4.2. The optical cycles

In this section we consolidate the data for nine seasons of APT observations of the cycles of γ Cas. For each season we have fit the data to a suitably modified sine curve. We started from the results of RSH02 that the mean light level, semi-amplitude, period may change during a season. In our graphical solutions we have permitted these parameters to float freely, but we left the time of zero phase fixed. We modified the period by introducing a fixed rate of change through a season, that is, by assuming that $\dot{\mathrm{P}}$ is a constant. The modified representation becomes:

$$m_v = m_o(t) + a(t)\, sin(\, [2\pi/\dot{P}]\; ln(1 + [\dot{P}/P_o]\; t) + \phi_o\,) \tag{1}$$

where a(t) and m_o(t) are linear representations in time. The logarithm in equation (1) supplies higher order terms beyond the first-order expansion term in $\dot{P}$ used by RSH02. This fact explains slight differences we have rederived for the 1999/2000 and 2000/2001 cycles. However, like RSH02, we find that the periods derived for these seasons are too imprecise to link the cycles of these two seasons by a simple linear interpolation. RSH02 also noticed that they were unable to interpolate linearly between the seasonal periods of 65 and 79 days for 1999 and 2000, respectively, without postulating phase changes between these seasons. Likewise, in the current analysis we have found other cases where a period generated from the data within a season fits the extrapolation from the previous season. In some cases these mismatches cannot be easily accommodated by assuming a smoothly increasing or decreasing period between the seasons. Because this may actually the rule, it is more appropriate to examine the behavior of the cycles within each observing season rather than potentially overlooking interesting physics implied by these anomalies.

Figure 5 shows our best modified sine curve fits to the 1997–2004 cycle data for the V filter. Results for the B filter are virtually the same, except that the amplitudes are slightly

smaller. We note also that these data are uncorrected for the small-amplitude, 1.2-day period discussed in the next section. Table 2 gives the corresponding parameters for each season, including the start and end mean magnitudes in our solution. All values are given in days (HJD) and magnitudes. Errors have been computed by investigating the values needed to give just unacceptable fits for each season and taking averages of the results. These errors have meaning only in the context of our models for individual seasons. The reader should note that a negative value for the dimensionless quantity $\dot{P}/P$ corresponds to a lengthening period. The mean full amplitude for the cycles in the V filter, computed as twice the sum in quadratures of the two semiamplitudes given in the table, is 0.0366 magnitudes. These amplitudes and the X-ray amplitude in Fig. 4 account for the $\Delta \mathrm{L}_x/\Delta V$ of 80 we have adopted. In constructing these fits we noticed the following departures from constant-amplitude fits:

- During at least two seasons, 1998/1999 and 2003/2004, the cycles are exponentially damped. Their damping constants are 50 days and 13 days, respectively. Surprisingly, the 2003/2004 light curve grows again exponentially to an even larger amplitude than it had at the beginning of the season. The damping and growth rates are both 13 days. It is further remarkable that little or no phase change occurs during this transition.

- The damping behavior could mislead one to interpret the lengths of some of the cycles to be about double their true values. Our discovery that the cycles can damp out, particularly near an extremum, suggests that the cycle lengths in γ Cas occur over a slightly more restricted range of about 60–90 days than recognized by RSH02. For example, the assignment of 55 days for the period of the 1998/9 was the unforeseen result of not appreciating the damping behavior.

- It is also likely (see Fig. 5) that the 1999/2000 season is affected by a similar, though longer, growth in amplitude as compared to the previous season. RSH02 found that cycle amplitudes can change from one year to the next. We see now that the timescale over which this occurs can vary significantly.

- Changes in the period can occur over intervals shorter than the period itself (RSH02's "change in phase"). Although in Fig. 5, we have represented the 1999-2000 cycles season by both a simple (but growing in amplitude) sine wave and one with an increasing period (dashed line), it is also possible to fit the data with a sine curve in which the phase seems to lag by 20–30 days at the minimum of the second cycle in this season.

- The periods can change in more complex ways than as represented by a single $\dot{P}$ term in equation (1). For example, the data in the 2002/2003 season can be fit adequately only by allowing the "period" to shorten and then lengthen during this interval. Thus,

neither the dashed nor solid-line representation, denoting a constant period or constant $\dot{P}$, respectively, can represent the obvious change in intervals between the three minima of this season.

- The mean magnitudes change slowly from season to season, for example undergoing variations from 2.171 to 2.188 magnitudes from 1998/9 to 1999/2000. These changes, together with growth/dampings of cycles, can produce ambiguities in the interpretation of the cycle length. For example, we are unable to model the variations during the 2005/6 season yet because we do not know how to interpret the mean magnitude for this season. The light curve at this time seems to undergo part of a long cycle but then to settle down to a short cycle length (≈50 days). Future monitoring may help resolve the evolution of the light curve when at least three cycle parameters change during a season.

An examination of these fitting parameters indicates no correlation among them, for example of amplitude with time, nor are they correlated with the yearly $\Delta B/\Delta V$ values or with the much longer V/R Hα emission data given by Miroschnichenko et al. (2002). It is much too early to be able to associate cycle attributes with one another.

Finally, we point out that RSH02 found the correlated optical/X-ray cycles from the 1999 and 2000 cycles in this plot. In addition, we note that the slightly low X-ray flux recorded during November 1998 (Robinson & Smith 2000) corresponds to the weak secondary minimum of the 1998/9 optical cycle shown in Fig.5.

4.3. The Viability of the Dynamo Model

The suggestion in RSH02 that the correlated variations in X-rays and optical emission are ultimately due to dynamo cycles in the decretion disk remains an attractive hypothesis. However, there are significant differences between the dynamics of this system and any of the current numerical simulations of disk dynamos in the literature. The bulk of the decretion disk mass, and most of its optical emission, comes from the inner regions of the disk, where the magnetic field of the star may be strong enough to enforce corotation out to at least $\sim 1R_*$ above the star's surface (RSH02). If one takes the characteristic density of the disk to be 10^{12-13} cm^{-3}, then the strength of the stellar magnetic field in pressure equilibrium with respect to the bulk kinetic (i.e., orbital) energy should be a few hundred Gauss near the corotation radius. This is consistent with a typical magnetic field strength at the stellar surface of more than 10^4 G (see §5.4) in a highly disordered field. On the other hand, a disk dynamo will be driven by the magneto-rotational instability (MRI), which will

saturate at a magnetic energy density less than the thermal pressure in the disk. This density corresponds to a magnetic field strength of ~ 10 G. Numerical simulations (for a review see Balbus & Hawley 1998) suggest that magnetic fields may fail to reach this limit by an order of magnitude, depending on the orientation of the field in the disk. Apparently, in the absence of mitigating factors, we might expect the stellar magnetic field to dominate over any plausible MRI dynamo field by a factor of roughly 100. Such a strong externally driven field would act to suppress the local MRI instability, although the global stability of the system is uncertain (Spruit, Stehle & Papaloizou 1995; Stehle & Spruit 2001). We conclude that unless arguments can be advanced that the stellar field is somehow excluded from the disk, for example by the stellar wind (see, e.g., ud Doula & Owocki 2000), its influence on the disk field could quench the MRI dynamo mechanism.

Despite this problem, it is still possible that long timescale variations in γ Cas are the result of disk instabilities. One possibility is that the dynamo mechanism may have little to do with the MRI dynamo. Instead, they may be a heretofore uncontemplated result of nonlocal interactions between the disk and the star. In either case it is clear that the available simulations of the disk dynamos are an unreliable guide to the dynamics of this system.

5. Discovery of a 1.2-day periodicity

5.1. Observational characteristics of a 1.2-day periodicity

The initial motivation to monitor γ Cas with the APT was to search for a signature of the rotational period. For a broad-lined, early B-type star on the main sequence, this period should be near one day. To search for such a period, we analyzed the nine individual seasons of our γ Cas observations with the method of Vaniĉek (1971). This procedure is based on least-squares fitting of sinusoids. Henry et al. (2001) and additional references therein describe how this method allows us to locate and fix individual frequencies in succession to determine all of the multiple frequency components present in a dataset. The Vaniĉek (1971) method differs from prewhitening for a given frequency before searching for the next by the investigator's fixing only the given frequency and not its amplitude, phase, or mean light level before computing a new power spectrum. The new frequency search is carried out while simultaneously fitting a single new mean brightness level along with the amplitudes and phases of all frequencies introduced as fixed parameters. In the resulting least-squares spectra, we plot the fractional reduction of the variance (reduction factor) versus trial frequency. This method holds an advantage over prewhitening, especially in the low-frequency domain, where mean light levels, amplitudes, and phases might be poorly de-

termined. Thus, it avoids perpetuating systematic errors in these parameters in successive searches for additional frequencies.

We applied this strategy to each of the nine seasons of our γ Cas photometry by searching the frequency range 0.001 to 2.5 day^{-1}, corresponding to a period range of 0.4 to 1000 days. In each season, for both the V and B datasets, we found evidence for a weak frequency near 0.8225 day^{-1}, or approximately 1.215 days, after fixing up to several low frequencies arising from the cycles discussed in §3.4 above. Due to the changing nature of the stronger cycles and the difference in the cadence of the observations from season-to-season (§2.1, above), the robustness of the 1.215 period we determined varied significantly from year to year.

As an additional check on the presence of the 1.215 day period, we repeated our period analysis on the combined season 2 through 9 datasets; season 1 was omitted from this analysis because of the undetermined offset of those observations (see §2.1, above). To our surprise, the 0.8225 day^{-1} frequency was clearly seen in the power spectrum of the complete dataset after fixing several of the strongest low frequencies, suggesting the possibility that the 1.215 day period remains *coherent* in phase throughout our entire 9 year dataset. The top panel of Fig. 6 shows the power spectrum of the season 2 through 9 V-filter observations after fixing the low frequencies 0.00838, 0.01225, 0.00103, and 0.00321 day^{-1}. The strongest remaining frequency, marked with the large arrow, is 0.82250 $\pm$0.00001 day^{-1}, corresponding to a period of 1.21580 $\pm$0.00002 days. The smaller arrows mark the $\pm$1 day aliases of the 0.82250 day^{-1} frequency. The small clusters of frequencies at 1 and 2 day^{-1} are the one day aliases of the residual low-frequency variations visible at the extreme left of the top panel that have not been fixed in this analysis. The bottom panel of Fig. 6 shows the results of fixing the previous four low frequencies *and* the 0.82250 day^{-1} frequency. There are no other frequencies in this range that appear significantly above the noise level. We repeated this analysis with the season 2 through 9 B-filter observations with nearly identical results. After fixing three low frequencies at 0.00837, 0.01222, 0.00383 day^{-1} in the B data, the strongest remaining frequency was 0.82249 $\pm$0.00001 day^{-1}, corresponding to a period of 1.21582 $\pm$0.00002 days. Thus, the mean period from the V and B datasets is 1.21581 $\pm$0.00001 days, and it is stable against removal of the low frequencies in both cases. An additional search for higher frequencies out to 30 day^{-1} was negative.

The top panel of Figure 7 plots the variations of all the V observations from seasons 2 through 9 after prewhitening for the four low frequencies mentioned in the above paragraph and phased with the 1.21581 day period and the arbitrary epoch HJD 2450000. A similar plot for the B observations is essentially identical. The peak-to-peak amplitudes of the 1.21581 day period in the V and B passbands, based on least-squares sine fits of the non-

prewhitened original datasets, were 0.0053 ±0.0004 and 0.0055 ±0.0004 mag, respectively. Thus, the amplitudes are identical within their uncertainties.

Inspection of Fig. 7 reveals that the waveform is highly nonsinusoidal. Indeed, the maximum occurs at phase ∼0.49, while the minimum is visible at about 0.71. Such an asymmetric waveform is unusual in astrophysical processes that generate a single oscillation. This property suggested that the waveform could be fit analytically by a Lehmann-Filhes solution, in the manner of fitting radial velocity solutions of a binary star. Then the functional form of the single-wave curve is given by:

$$m \;=\; K\,cos(\phi+\omega) + e\,cos(\omega). \tag{2}$$

Here m represents the apparent magnitude rather than a radial velocity, and K, ϕ, e, and ω can be thought of as analogs of the orbital parameters velocity semi-amplitude, phase, eccentricity, and longitude of periastron. The latter quantity is an arbitrary phase zeropoint similar to our arbitrary photometric epoch of JD 2450000. We verified the aptness of this functional fit by binning the phase curves into 100 bins (0.01 cycles) and overplotting the 0.01-cycle means with the solution. This is shown in the bottom panel of Fig. 7. No systematic departures of the binned data could be discerned with respect to the solution in either dataset, further suggesting that the 1.21581 day period is coherent throughout our dataset. For the B filter our solution is K = 0.00300±.00013 mags, e = 0.333±0.049, and ω = 280.3±9.9, while for the V filter it is K = 0.00302±.00013 mag, e = 0.372±0.052, and ω = 289.6±9.7. Since this waveform is to be preferred over the sinusoidal representation, the derived K values should be regarded as the true semi-amplitudes of the variation. We also note the remarkable fact that the K_B/K_V ratio is 1.00±0.007.

As a final check on the long-term amplitude and phase coherency of the 1.21581 day period, we fit least-squares sinusoids at that period to the non-prewhitened data in the individual observing seasons 2 through 9 (1998/9–2005) independently. Table 3 lists the resulting peak-to-peak amplitudes in V and phases of minimum for the eight observing seasons in columns 2 and 3, respectively, along with their individual formal errors. Notice that standard deviations of the amplitudes and phases are 0.0030 mag and 0.074 phase units, respectively, both significantly larger than the typical formal errors. This could suggest conceivably that there are season-to-season variations in amplitude and phase and, thus, some degree of non-coherency in the 1.21581 day period. However, as noted earlier, the natures of the cycles and the cadences of the observations are significantly different from season to season. This situation could result in systematic errors in the amplitudes and phases that would render the formal errors too small. To test this hypothesis, we removed (prewhitened) the 1.21581 day period from the season 2 through 9 V light curves and added

a similar but randomly chosen 1.1976 day coherent variation with the same amplitude as the 1.21581 day period. We then repeated the sine curve fits for the individual seasons using the artificial 1.1976 day period. The results are given in columns 4 and 5 of Table 3. The standard deviations of the amplitudes and phases of the artificial 1.1976 day period are 0.0025 mag and 0.089 phase units, similar to our results with the 1.21581 day period and also larger than the typical formal errors. Therefore, this result is consistent with the amplitude and phase stability of the 1.21581 day period throughout our complete dataset. This addresses the disparity between the "sigma" in the table and the formal photometric errors.

5.2. The rotational nature of the 1.2-day period

Three possible explanations present themselves for a coherent 1.2 day period in an early B star: rotation, ellipsoidal variation, and (nonradial) pulsation. Among these, rotation is by far the most likely mechanism, primarily because it is well within the narrow range of rotational periods suggested for this star. The rotational period can be determined by knowing the rotational velocity, radius, and rotational obliquity, i. Recent values of the rotational velocity are 400 $\mathrm{km\,s^{-1}}$ and 432 $\mathrm{km\,s^{-1}}$ (Harmanec 2002, Zorec, Frémat, & Cidale 2005), the mass and log gravity are $15.2\pm0.9\mathrm{M}_\odot$ and 3.80, respectively. As already mentioned, values of i ranging from 46^o to 60^o have been determined from interferometry. This range of parameters gives an expected range for the rotational period of 1.08–1.41 days. The mean of these is 1.245 days, which is close to the 1.21581 period from our APT photometry. However, before accepting rotation as the driver of this variation, we consider the competitive explanations.

One may dismiss readily the possibility that the 1.2 day period arises from an ellipsoidal variation of the Be star in a 2.4 day orbit. Such a variation could only arise in a binary with comparable component masses in a close system. It would produce a radial velocity variation, $2K$, of tens of $\mathrm{km\,s^{-1}}$, which would have been easily observed, e.g., in the data of Harmanec et al. (2000) and Miroschnichenko et al. (2002). In addition, a 2.4-day system would be tidally locked for a main sequence B star. The photospheric line profiles are much too broadened to arise from a star having this long a rotational period.

Arguments against nonradial pulsations are also strong, but not as clear cut. Empirically, we know that NRPs in B stars are often multiperiodic. This circumstance has opened up the new field of asteroseismology in massive stars. However, the best examples of pulsations in massive stars hotter than the short-period β Cep stars, namely ζ Oph and HD 93521 (Reid et al. 1993, Howarth & Reid 1993), indicate that the pulsations in these stars have periods of only several hours. A stronger, theoretical argument is that the NRP periods of

B stars are *predicted* to decrease with T_{eff} because their values should be of the order of the thermal timescale in the Z-bump driving zone where the pulsations are excited (e.g., Pamyatnykh 1999). These timescales for ∼B0.5 IV stars are only several hours and therefore appear incompatible with the 1.2 day period.

Additional (in our view, clenching) arguments against NRP are the complete absence of color variation in our well constrained determination of the $\Delta B/\Delta V$ ratio and the nearly saw-tooth waveform. To our knowledge this flux ratio is grayer than any known variation among BAF-type pulsating stars. In contrast, variations imposed by low-frequency (co-rotating frame!) NRP modes in B stars show a color variation (e.g., De Cat et al. 2005), and this is consistent with theoretical predictions that a color term should be generated in the flux variations. In addition, the waveform exhibited by NRP variables across the H-R Diagram is universally close to sinusoidal.

5.3. Previous claims of a rotational period

The present period is at variance with several claims of a rotational period for γ Cas in the literature. These include claims by Harmanec (1999) of a spectroscopic period. More perplexing are reports by Marchenko et al. (1998) and Harmanec et al. (2000) of a total of 3 periods in the range of 1.04–1.64 days in the *Hipparcos* (Perryman et al. 1997) light curve. In addition, SRC98 and SRH98 found a period of 1.123 days from *RXTE* and *IUE* fluxes. We discuss each of these as follows.

Harmanec (1999)'s estimate of 1.16 days, close to our own, was based on the assumption that the acceleration of msf's in optical line profiles is due to fixed disturbances on the star's surface. This value, unlike ours, is subject to uncertainties in the estimated inclination and radius of the star, and especially to the distance of the clouds responsible for msf's above the star's surface. placement of the msf disturbances on the star's surface. His result can be expected to be imprecise, but rather close to our own, as indeed it is.

We have repeated the analysis of Marchenko et al. (1998) Harmanec et al. (2000). We agree with the latter authors that the *best candidate period* in the *Hipparcos* light curve is 1.487 days, However, when the dataset is broken into two and three segments, this signal was found to be confined to the middle segment and therefore cannot be described as a coherent period. From our examination of this light curve, we conclude that no coherent periods near 1 day can be reliably found. The principal problem is that the *Hipparcos* data are too sparse and poorly sampled to resolve the long-term, low-amplitude (3%) 60–90 day irregular cycles in γ Cas. It appears that the short periods derived by these authors are likely to be aliases

of these cycles. Our conclusion is confirmed by our experience with comparisons of other extended APT datasets and corresponding *Hipparcos* light curves. For example, Henry et al. (2000) have used comparable quality APT data for a large sample of stars, many of which were found to be variable with full amplitudes as low as 0.6%. These same stars were also observed by *Hipparcos.* Variability was generally not found in the latter light curves when the amplitudes were less than 3%. Similarly, Henry & Fekel (2002a, 2002b) used APT data to discover periods in 6 new γ Dor and 5 δ Scu variables, respectively. Only two of these stars showed indications of variability in the *Hipparcos* data. However, because two-channel photometers were used, this probably slightly overstates the relative APT advantage.

The 1.21 day period likewise contradicts the SRH98 claim of a period near 1.12 days. This claim was based from bootstrapping from an initial rough (and nonunique) estimate obtained from an analysis of UV continuum dips in a 1.2 day time series of *IUE* observations. SRC98's supposed that these dips correspond to repeating X-ray maxima over many rotations. Based on their search for recurring marker in a series of 6 1.1-day *RXTE* observations, RSH02 concluded that such markers may disappear within a week, or about 6 rotation cycles. Indeed, this discovery undermined a key assumption made in deriving the SRH02 period.

5.4. The origin of the periodicity

Explanations for the origin of this period are not yet well constrained, but there is perhaps enough information to point us in the right direction. Possible locations of the origin of the rotational signature are the surface of the star and a co-rotating structure just above some point above the stellar surface. The sawtooth waveform presents a difficulty for either case. The circumstellar explanation at first seems attractive because we know that such clouds exist. The absence of a color variation means that the continuum-emitting clouds would have to have the photospheric temperature and thus be close to the star. In this picture, the fact that the light level falls below the maximum during most of the cycle would mean that emitting clouds are distributed over a range of stellar longitudes and are occulted as they co-rotate behind the star. This requirement for proximity to the surface forces the circumstellar explanation to posit the existence of many small dense sources corotating over points on the surface with a range of longitudes. These sources would also have to be optically thick in the continuum, and this requires a column density of at least 10^{25} cm^{-2}. This requirement exceeds by two or three orders of magnitude the thick component of a two-density model of small circumstellar clouds discussed by Smith & Robinson (1999), based on their analysis of the variable Si IV and S IV line absorptions. While this is not impossible,

there is no support for continuum reemission from the cloud properties, for example, from the flatness of the 1996 March *GHRS* light curve between its obvious dips. These arguments cast doubt on a circumstellar origin for the variations in the optical light curve.

The explanation we favor is one in which a structure is firmly rooted within the star's envelope and is visible to observers at the surface. To date, we are aware of only one other early-to-mid B-type star, HD 37776, that exhibits rotational modulations (period = 1.538675 days; Adelman 1997) in unpolarized optical-continuum light.[3] This star is special even among Bp stars cause of its especially strong dipolar field strength (60 kG). The dipole coexists with a quadrupolar component that is nearly antialigned with the primary dipole (Thompson & Landstreet 1985, Khokhlova et al. 2000). The ensemble produces a double wave light curve. In the visible/red bandpasses the presence of the secondary flux bump is suppressed, with the result that the light curve takes on a quasi-sawtooth waveform (Mikulasek et al. 2006). The star has a heterogeneous surface distribution of the metals, and this appears to be the source of the light curve variations (Khokhlova et al. 2000).

The example of HD 37776 suggests that large and multi-polar magnetic fields on an early-type B star can produce its observed photometric variations over the rotational period. The amplitude of the visible wavelength light curve is about 3.3× larger than the variations we have reported for γ Cas. A simplistic scaling of the photometric amplitude ratio of HD 37776 with respect to γ Cas would likely lead to an overestimate of its mean surface field strength. Indeed, the details of the magnetic topology dominate such estimates and preclude a ready estimate of the maximum field strength.

In view of these arguments, we believe the best explanation for the monochromatic variations of γ Cas is that they are produced by an undiscovered strong multipolar field rooted on magnetic poles that are distributed over a range of stellar longitudes. (We emphasize once again that due to the broad lines of this star's spectrum, complicated by emission, an actual field is not likely to be detected for some time). The requirement that the fields be multipolar and distributed across the surface, is supported by the broad distribution of X-ray active maxima occurring over several 27-hour long X-ray monitoring campaigns (essentially the rotational period) of γ Cas (e.g., RSH02). Indeed, the instances of high X-ray activity are so numerous that it is possible only to discover *inactivity* markers by cross-correlating reciprocal X-ray flux curves (Robinson & Smith 2002, RSH02). Finally, the absence of a single

[3]By this statement we are excepting the case of the B2p star σ Ori E, which also exhibits continuum light variations (Hesser, Moreno, & Ugarte 1977). The difference is that its photometric variations are the result of absorption from an intervening corotating cloud (Smith & Groote 2001). In contrast, the photometric variations in HD 37776 are well correlated with strengths of spectral lines, also arising from high excitation potentials, e.g., by Khokhlova et al. (2000), and these cannot arise in an unheated circumstellar cloud.

dominant dipolar field is suggested by the lack of evidence of a magnetically focused wind, i.e., modulated low-velocity emissions and absorptions of UV resonance lines (e.g., Shore & Brown 1990), In contrast, these variations are the rule among well-observed magnetic Bp stars.

6. Conclusions

However well studied, γ Cas has become a prototypical astronomical onion, with each new discovery raising many more questions than answers about the interaction of complex processes in hot unevolved stars. In broad strokes, we can summarize the phenomenology relating to the complicated circumstellar environment by the following description.

A number of recent studies of γ Cas, including the simultaneous *RXTE–GHRS* campaign of 1996, have shown that in addition to the continuum flux, the strengths of a number of UV absorption lines are strongly correlated (or anti-correlated) with X-ray flux. Altogether, there are at least three systems of circumstellar debris: the (mainly) keplerian orbiting disk, the co-rotating clouds of various temperatures (visible in the UV continua or in the UV and optical as migrating subfeatures), and redshifted blobs moving at least roughly toward the star. There is therefore no need to invoke an association of any of the UV and the X-ray activities with the secondary star of the γ Cas binary system. Indeed, the variable ultraviolet diagnostics we found can be expected to be associated with the wind or disk of the Be star, and the X-ray fluxes are in turn correlated with them (Smith & Robinson 1999, Robinson & Smith 2000).

The evidence for a correlation between X-ray and optical cycles continues to accumulate, as in our Fig. 4. This seems to suggest that the X-ray production is ultimately tied to properties of a magnetized decretion disk. This argument, along with a noncorrelation of epochal X-ray fluxes with respect to the 204-day binary period, led RSH02 to suggest that a mechanism in the disk controls the conditions for hard X-ray production. However, this does not mean that this flux is emitted in this structure. In fact, the rapid evolution of flares is consistent only with densities of $\geq 10^{14}$ cm^3. This fact led SRC98 to place them on the surface of the star. The data used in this study is adequate to show that flare aggregates cannot trigger a response at visible wavelengths. SRC98 came to a similar conclusion based on uncorrelated X-ray and ultraviolet continuum fluxes.

A major unresolved issue in our understanding of the correlated X-ray and optical cycles is the possible role of a decretion disk dynamo. If the star's magnetic field intersects the stellar disk, it can be expected to quench an MRI disk dynamo. Perhaps the wind's outward

flow prevents the field from crossing the disk plane. According to the geometry of strong stellar winds in magnetic stars, this seems likely to some extent (see Smith & Fullerton 2004, Gagné et al. 2005). At some distances from the star, the wind finally dominates the field and opens outwards toward infinity. Thus, the flow and the field lines no longer penetrate the disk efficiently. Under these circumstances perhaps a dynamo can survive. The intermediate-timescale variations are equally puzzling. Are they evidence for spatially local structures which decouple from an otherwise interconnected magnetosphere/decretion disk system? Or, despite the similarity of their X-ray/optical scaling with the scaling of the long cycles, is the optical flux emitted from somewhere else, such as individual plasma clouds in the magnetosphere?

The most important result of this paper is the discovery of a coherent 1.2-day periodicity in both the B and V filters. The determination of The determination of a coherent period clearly moves the production of the X-rays one step closer to the intrinsic properties of the Be star. Like the larger optical variations of the multi-order magnetic B2p star HD 37776, the modulation in the γ Cas light curve has no accompanying $B - V$ color term. Our linking the γ Cas and HD 37776 variations together implies that γ Cas may yet turn out to be chemically peculiar and therefore an (albeit complex) member of the Bp class. However, helium is thought to remain closely coupled to hydrogen particles in winds of the hot stars (e.g., Hunger & Groote 1999). It is not yet clear whether a mechanism exists to segregate and distribute helium atoms over a star as hot as γ Cas. Accordingly, it may be productive to undertake a search for helium line strength modulations around the 1.2-day period. Such a test, e.g. of He I λ4471 (wholly in absorption), would provide an important means by which to establish whether helium rich patches associated with the early-Bp star can be found in stars hotter than the canonical limit (type B2) of this class.

It is likely that the B0.5–B1 IV star HD 110432 is a new member of the γ Cas "class" (Smith & Balona 2006). In addition to this star, Motch et al. (2005) have suggested the addition of four new members to the group. According to our picture, a γ Cas star requires a dense disk, magnetic field (probably complex), and a rapid rotation. The rapid rotation is necessary to insure the production of magnetic stresses between the star and the inner region of the Be disk where the rotation law transitions from corotation to keplerian. The high-order field is an additional (empirical) requirement, based on the absence of rotationally modulated UV resonance lines and Hα emission. These periodic emissions/absorptions over a cycle have proved to be reliable spectroscopic hallmarks of dipolar magnetic Bp stars. The requirement of rapid rotation and a magnetic field may also mean that γ Cas stars exist near the end of their main sequence evolution stage. This speculation emerges from growing evidence that magnetic fields and CNO-processing products (including He-enhancement) are correlated in evolved stars (Neiner et al. 2003, Lyubimkov et al. 2004, Huang & Gies 2006).

If additional abundance determinations of evolved stars confirm this initial trend, γ Cas analogs could be absent in very young clusters because not enough time has elapsed to bring their fields to the surface.

We thank Mr. Lou Boyd for his continuing support of the automatic telescopes at Fairborn Observatory and Dr. Frank Fekel for providing the Lehmann-Filhes fit to the phase curve in Fig. 7. We also want thank Dr. David Bohlender for pointing out the importance of HD 37776 for the context of this paper. It is also a pleasure to thank both Dr. Steve Cranmer and an anonymous referee for suggestions that improved this paper. This work was supported by NASA grant NNG05GB60C to the Catholic University of America and by NASA grant NCC5-511 and NSF grant HRD 97-06268 to Tennessee State University.

REFERENCES

Adelman, S. J. 1997, A. & A. Suppl., 125, 65

Berio, P., Stée, Ph. 1999, A. & A., 345, 203

Breger, M. 1974, ApJ, 188, 53

de Cat, P. Briquet, M., et al. 2003, A. & A., 452, 1013

Gagné, M., Oksala, M. E. et al. 2005, ApJ, 628, 986

Hunger, K., & Groote, D. 1999, A. & A., 351, 554

Harmanec, P. 1999, A. & A., 341, 867

Harmanec, P., Habuda, P. et al. 2000, A. & A., 364, 85

Harmanec, P. 2002, Exotic Stars as Challenges to Evolution, ed. C. A. Tout & W. van Hamme, ASP Conf. Ser., 279, 221

Henry, G. W. 1995a, in ASP Conf. Ser. 79, Robotic Telescopes: Current Capabilities, Present Developments, and Future Prospects for Automated Astronomy, ed. G. W. Henry & J. A. Eaton (San Francisco: ASP), 37

Henry, G. W. 1995b, in ASP Conf. Ser. 79, Robotic Telescopes: Current Capabilities, Present Developments, and Future Prospects for Automated Astronomy, ed. G. W. Henry & J. A. Eaton (San Francisco: ASP), 44

Henry, G. W., Fekel, F. C., Henry, S. M., & Hall, D. S. 2000, ApJS, 130, 201

Henry, G. W., Fekel, F. C., Kaye, A. B., & Kaul, A. 2001, AJ, 122, 3383

Henry, G. W., & Fekel, F. C. 2002a, PASP, 114, 988

Henry, G. W., & Fekel, F. C. 2002b, PASP, 114, 999

Hesser, J. E., Moreno, H., & Ugarte, P. 1977, ApJ, 216, L31

Hony, S., Waters, L. B., Zaal, P. A. et al. 2000, A. & A., 355, 187

Horaguchi, T., Kogure, T. et al. 1994, PASJ, 46, 9

Howarth, I. & Reid, A. H. N. 1993, A. & A., 279, 148

Huang, W. Gies, D. R. 2006, ApJ, submitted (astro-ph/0510720)

Hummel, W. 2000, The Be Phenomenon in Early-Type Stars, ed. M. Smith, H. Henrichs, & J. Fabregat, ASP. Conf. Ser., 214, 396

Khokhlova, V. L., Vasil'Chenko, D. V., Stepanov, V. V. & Romanyuk, I. I. 2000, Ast. Let., 26, 177

Krticka, K., Mikulasek, Z., Zverko, J., & Ziznovsky, J. 2006, Active OB Stars: Laboratories for Stellar & Circumstellar Physics, ed. S. Stefl, S. Owocki, & A. Okazaki, ASP Conf. Ser., in press

Lyubimkov, L. S., Rostopchin, S. I, & Lambert, D. L. 2004, MNRAS, 351, 745

Marchenko, S. V., Moffat, A. F. J. et al. 1998, A. & A., 331, 1022

Mikulasek, Z., Krticka, J., et al. 2006 Active OB Stars: Laboratories for Stellar & Circumstellar Physics, ed. S. Stefl, S. Owocki, & A. Okazaki, ASP Conf. Ser., in press

Millar, C., & Marlborough, J. M. 1998, ApJ, 474, 715

Miroschnichenko, A., Bjorkman, K., & Krugov, V. 2002, PASP, 114, 1226

Motch, C., Lopes de Oliveira, R., Negueruela, I., Haberl, F., & Janot-Pacheco 2006, Active OB Stars: Laboratories for Stellar & Circumstellar Physics, ed. S. Stefl, S. Owocki, & A. Okazaki, ASP Conf. Ser., in press

Neiner, C., Hubert, A.-M., et al. 2003, A. & A., 409, 275

Okazaki, A. T. & Negueruela, I. 2001, A. & A., 377, 161

Pamyatnykh, A. 1999, Acta Astr., 49, 119

Pedersen, H., & Thomsen, B. 1977, A. & A. Suppl., 30, 11

Perryman, M. 1997, The Hipparcos and Tycho Catalogues, ESA SP-1200 (Noordwijk: ESA)

Quirrenbach, A., Bjorkman, K. et al. 1997, ApJ, 479, 477

Reid, A. H. N., Bolton, C. T. et al. 1993, ApJ, 417, 320

Robinson, R. D. & Smith, M. A. 2000, ApJ, 540, 474

Robinson, R. D. & Smith, M. A., & Henry, G. W. 2002, ApJ, 575, 435

Smith, M. A. & Balona, L. A. 2006, ApJ, 640, 491

Smith, M. A. & Groote, D. 2001, A. & A., 372, 208

Smith, M. A. & Huang, L. 1994, Pulsation, Rotation, & Mass Loss in Early-Type stars, ed. L. Balona, H. Henrichs, & J. LeContel (Dordrecht: Kluwer), p. 37

Smith, M. A., 1995, ApJ, 442, 812

Smith, M. A., Cohen, D. H. et al. 2004, ApJ, 600, 972

Smith, M. A. & Robinson, R. D. 1999, ApJ, 517, 866

Smith, M. A., & Robinson, R. D. 2003, in ASP Conf Ser. 292, Interplay between Periodic, Cyclic, and Stochastic Variability, ed. C. Sterken (San Francisco: ASP), 263

Smith, M. A., Robinson, R. D., & Corbet, R. H. D. 1998, ApJ, 503, 877

Smith, M. A., Robinson, R. D., & Hatzes, A. P. 1998, ApJ, 507, 945

Smith, M. A., Robinson, R. D., & G. W. Henry 2002, ApJ, 575, 435

Smith, M. A., & Robinson, R. D. 2003, in ASP Conf Ser. 292, Interplay between Periodic, Cyclic, and Stochastic Variability, ed. C. Sterken (San Francisco: ASP), 263

Spruit, H.C., Stehle, R., & Papaloizou, J.C.B. 1995, MNRAS, 275, 1223

Stehle, R., & Spruit, H.C. 2001, MNRAS, 323, 587

Thompson, I. B., & Landstreet, J. D. 1985, ApJ, 289, L9

Tycner, C., Haban, A. R. et al. 2004, AJ, 127, 1194

ud Doula, A., & Owocki, S. P. 2002, ApJ, 576, 413

Vaniĉek, P. 1971, Ap & SS, 12, 10

Waters, L. B., Coté, J., & Lamers, H. J. 1987, A. & A., 185, 206

Yang, S., Ninkov, Z., & Walker, G. A. 1988, PASP, 100, 233

Zorec, J., Frémat, Y., & Cidale, L. 2005, A. & A., 441, 235

Figure Captions

Fig. 1.— The m_V, m_B scatter plot for APT observations of γ Cas during the 2000/2001 and 2001/2002 seasons. The regression lines shown as dashed and solid lines have slopes that differ from one another at a significance level of 2.4 sigma.

Fig. 2.— The sequence of *RXTE/PCA* fluxes (dots) and m_v magnitudes (crosses) for γ Cas on 2004 November 9 (HJD 2453318). Error bars for the two types of observations are shown. Asterisk symbols represent the X-ray data binned to the same sampling rate as the APT data (crosses), or about 10 minutes. The analysis of simultaneous data discussed in the text concerns the paired asterisks-crosses shown.

Fig. 3.— The relative B and V magnitude light curve on the nights of 2003 November 19 and 20 (Julian Dates 2452962–3), shown as squares and dots respectively (zeropoints are arbitrary). The dashed curves are linear regression fits to the data.

Fig. 4.— The *RXTE*/PCA light curve for γ Cas for our program. Each dot represents a 16-second integration. The scatter is due to rapid flaring and to slow chaotic undulations; the errors in the observations, shown in the top left, are very small by comparison. Time-zero refers to 2004 November 05.0 (i.e., HJD 2453314.5). The dashed line is the *predicted* cyclical behavior of the X-ray flux based of the contemporaneous 85 day optical cycle determined by the robotic Automated Photometric Telescope system located in Arizona. This curve was computed from the X-ray/optical relation over several cycles found by Robinson, Smith, & Henry (2002). *No* time or flux adjustments have been made in its representation.

Fig. 5.— Cycles for 1997-2004 seasons. Dashed lines denote alternative (constant period) solutions or an undamped fit (panel g). The comb at the bottom of panel h shows the time interval of simultaneous APT–*RXTE* observations. The magnitude scale on each of the figures is the same except for season 2003/4. As in other representations, the magnitude zero is uncertain for season 1997/8.

Fig. 6.— *Top* : Power spectrum of the season 2 through 9 V-observations after fixing the low frequencies 0.00838, 0.01225, 0.00103, 0.00321 day^{-1}. The ordinate is the fractional reduction of the variance. The strongest remaining frequency, marked with the large arrow, is 0.82250 $\pm$0.00001 day^{-1}, corresponding to a period of 1.21580 $\pm$ 0.00002 days. The smaller arrows mark the $\pm$1 day aliases of the $\pm$0.82250 day^{-1} frequency. *Bottom* : Power spectrum showing the results of fixing the four low frequencies *and* the 0.82250 day^{-1} frequency. There are no other frequencies in this range that appear significantly above the noise level, except for the one day aliases of remaining low-frequency variation.

Fig. 7.— *Top* : Season 2 through 9 photometric V observations phased with the 1.21851 period and the arbitrary epoch HD 2450000. The data have been prewhitened to remove the low frequencies given in the text; the mean is also removed. The solid line is the fit for a "Lehmann-Filhes" function (equation 2). *Bottom*: Data from the top panel averaged into 100 phase bins and plotted with an expanded scale for the y axis. Error bars give the standard deviations of the mean for each bin. The solid curve is the same one in the top panel. The binned data show good conformance to the now more discernible mean curve.

Table 1. PHOTOMETRIC OBSERVATIONS OF γ Cas

Date (HJD − 2,400,000)	Var B (mag)	Var V (mag)	Chk B (mag)	Chk V (mag)
50711.7151	99.999	99.999	−0.822	99.999
50718.6966	−4.393	−3.641	−0.818	−1.216
50718.9253	−4.393	−3.642	−0.814	−1.222
50720.7936	−4.386	−3.644	−0.821	−1.218
50720.9191	−4.387	−3.638	99.999	−1.223
50721.6940	99.999	−3.648	99.999	99.999

Note. — Table 1 is presented in its entirety in the electronic edition of the *Astrophysical Journal* and at http://schwab.tsuniv.edu/t3/gammacas/gammacas.html. A portion is shown here for guidance in data format and content.

Table 2: Cycle Fit Parameters to Two Sinusoids*

Year	P_o	$\dot{P}/P$	a_1	a_2	$< m_v(start) >$	$< m_v(end) >$	t_o - HJD2400000
1997/8	61	0.0	0.009	0.011	2.165	2.160	50750.2
1998/9	65	0.0	0.020	$\sim$0	2.134	2.170	51145.7
1999/0	72	-2.4×10^{-4}	0.008	0.0015	2.147	2.147	51311.2
2000/1	91	0.0	0.012	0.0012	2.143	2.143	51825.0
2001/2	73	1.5×10^{-5}	0.012	0.007	2.142	2.132	52123.3
2002/3	80	-1.0×10^{-5}	0.0125	0.0125	2.1365	2.138	52521.8
2003/4	80	0.0	0.021	0.031	2.137	2.128	52805.5
2004/5	85	0.0	0.013	0.013	2.1362	2.1377	53197.5

*Errors: δP = $\pm$2 days, Fractional $\dot{P}/P = \pm20\%$, a_1, a_2 = $\pm$0.001mags., $< m_v >$ =$\pm$0.002 mags., t_o = $\pm$3 days.

Table 3. Sinusoidal Fits to 1.2 day Periods in Yearly γ Cas Observations

Year	P = 1.21581 Peak-to-Peak Ampl. (mag)	P = 1.21581 Phase of Minimum (phase units)	Control: P = 1.1976 Peak-to-Peak Ampl. (mag)	Control P = 1.1976 Phase of Minimum (phase units)
1998/9	0.0066 ± 0.0015	0.921 ± 0.036	0.0085 ± 0.0015	0.242 ± 0.028
1999/0	0.0066 ± 0.0015	0.818 ± 0.036	0.0109 ± 0.0015	0.256 ± 0.022
2000/1	0.0028 ± 0.0018	0.775 ± 0.091	0.0061 ± 0.0017	0.170 ± 0.042
2001/2	0.0095 ± 0.0014	0.848 ± 0.023	0.0071 ± 0.0014	0.374 ± 0.030
2002/3	0.0053 ± 0.0017	0.816 ± 0.048	0.0075 ± 0.0016	0.211 ± 0.035
2003/4	0.0040 ± 0.0012	0.783 ± 0.044	0.0039 ± 0.0012	0.425 ± 0.045
2004/5	0.0112 ± 0.0009	0.985 ± 0.013	0.0051 ± 0.0010	0.235 ± 0.030
2005/6[a]	0.0026 ± 0.0042	0.024 ± 0.267	0.0106 ± 0.0042	0.194 ± 0.063
Sigma	0.0030	0.074	0.0025	0.089

[a]Partial season through July analyzed with only 31 observations.

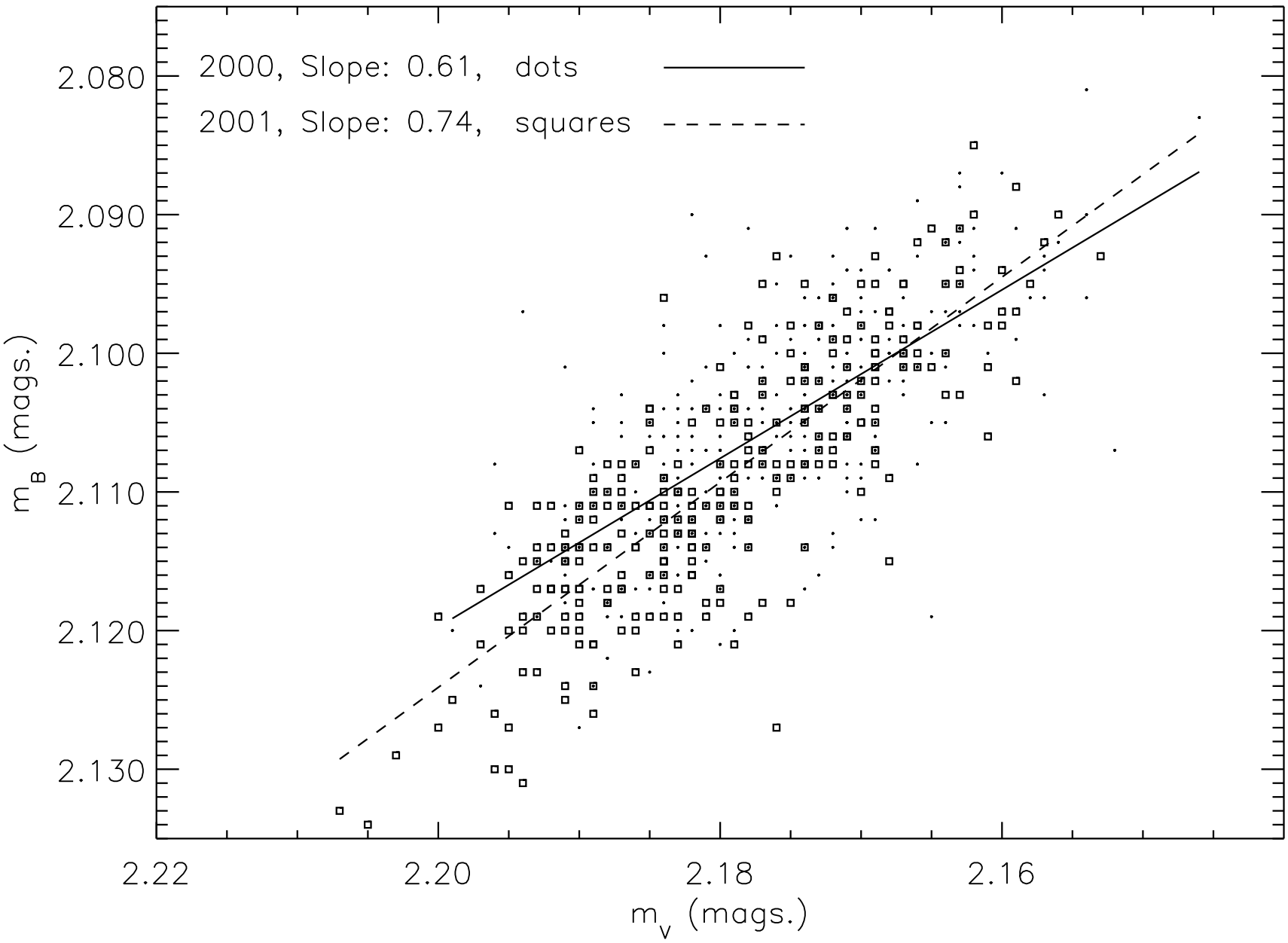
2000, Slope: 0.61, dots
2001, Slope: 0.74, squares
2.080
2.090
2.100
2.110
2.120
2.130
m_B (mags.)
2.22
2.20
2.18
2.16
m_V (mags.)

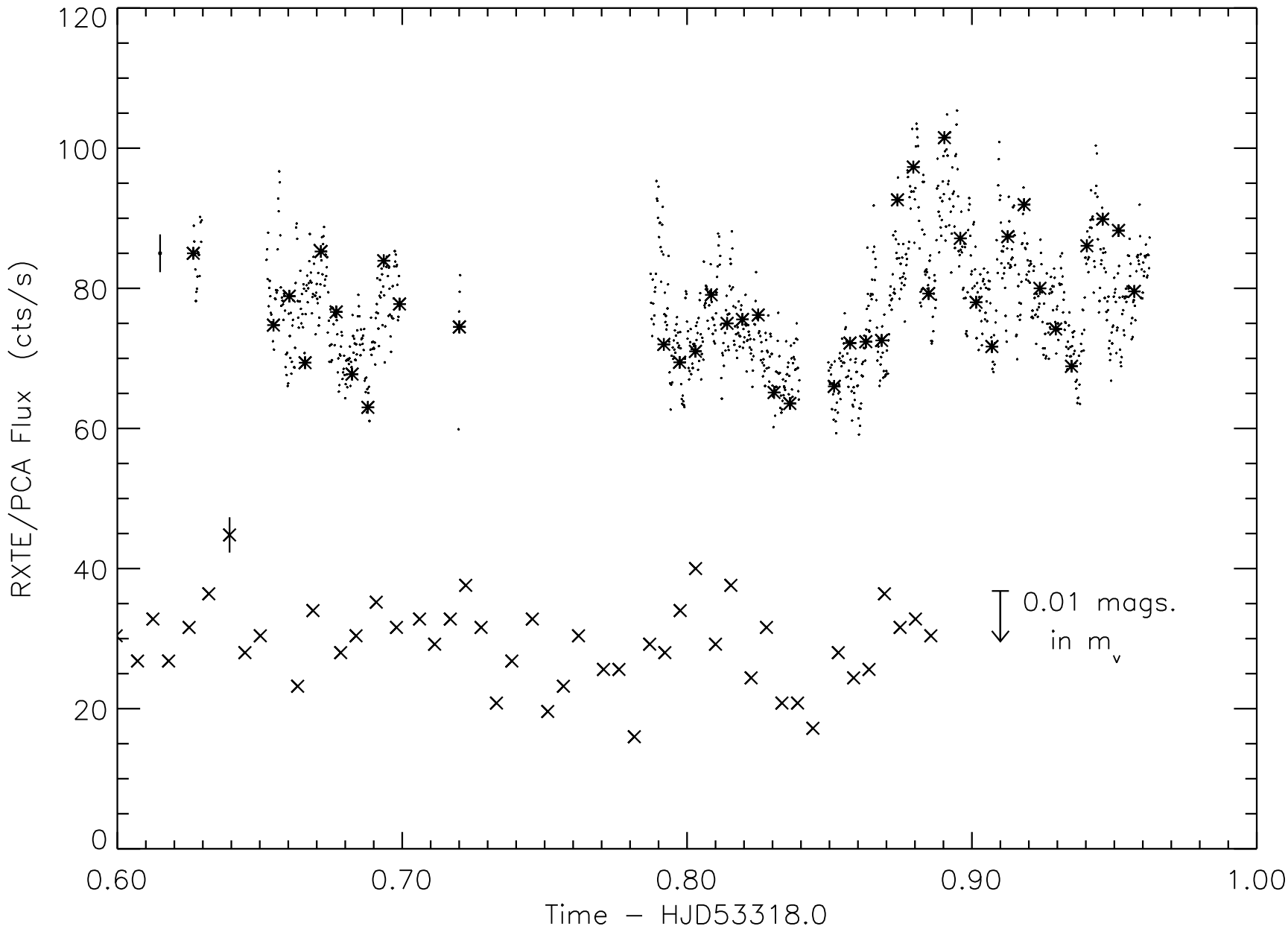
120
100
80
60
40
20
0
RXTE/PCA Flux (cts/s)
0.60
0.70
0.80
0.90
1.00
Time − HJD53318.0
0.01 mags.
in m_v

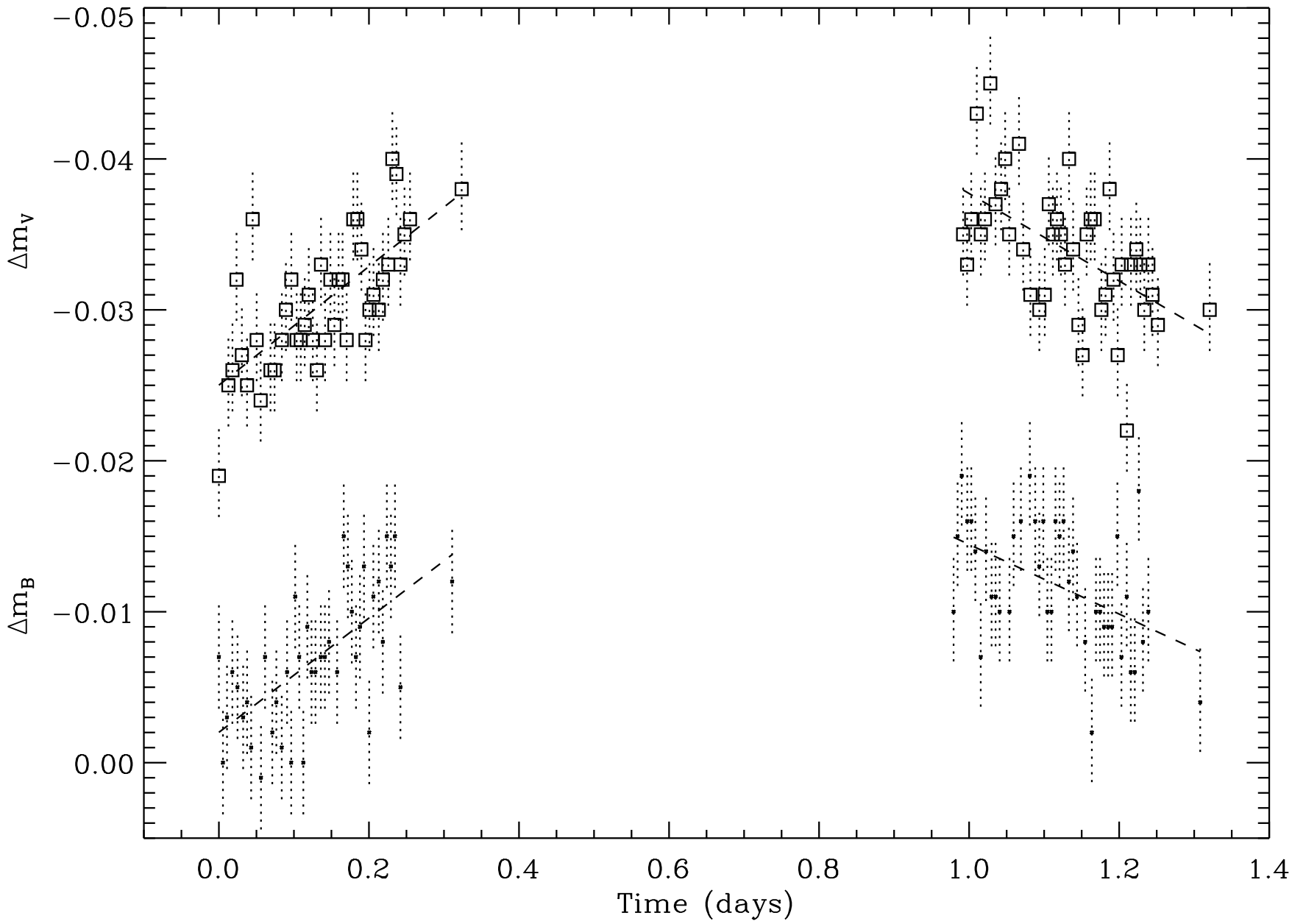
−0.05
−0.04
−0.03
−0.02
−0.01
0.00
Δm_V
Δm_B
0.0
0.2
0.4
0.6
0.8
1.0
1.2
1.4
Time (days)

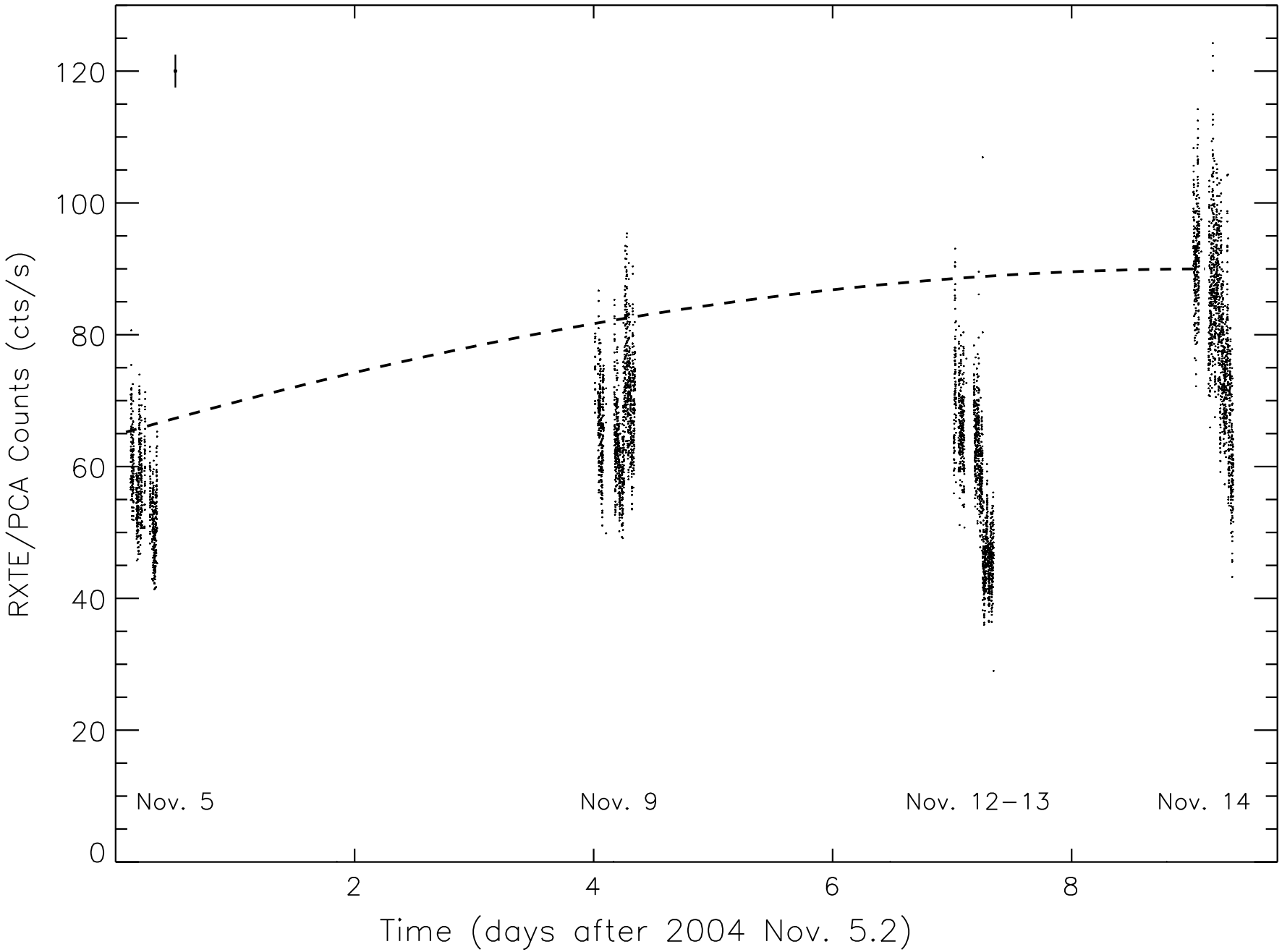
RXTE/PCA Counts (cts/s)
0
20
40
60
80
100
120
2
4
6
8
Time (days after 2004 Nov. 5.2)
Nov. 5
Nov. 9
Nov. 12−13
Nov. 14

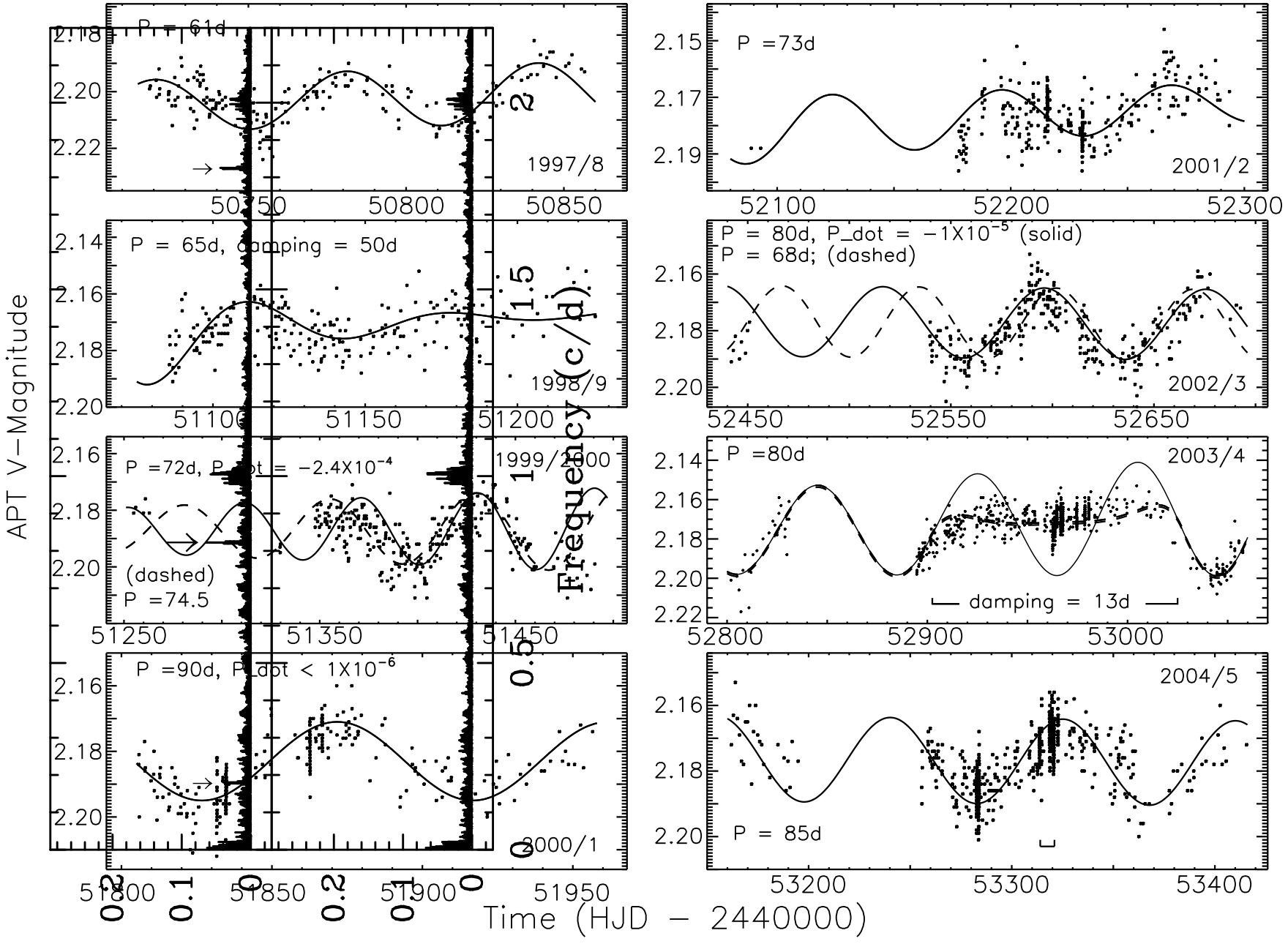
P = 61d
1997/8
P = 65d, damping = 50d
1998/9
P =72d, P_dot = −2.4X10^−4
(dashed)
P =74.5
1999/2000
P =90d, P_dot < 1X10^−6
2000/1
P =73d
2001/2
P = 80d, P_dot = −1X10^−5 (solid)
P = 68d; (dashed)
2002/3
P =80d
damping = 13d
2003/4
2004/5
P = 85d
APT V−Magnitude
Frequency (c/d)
Reduction Factor
Time (HJD − 2440000)

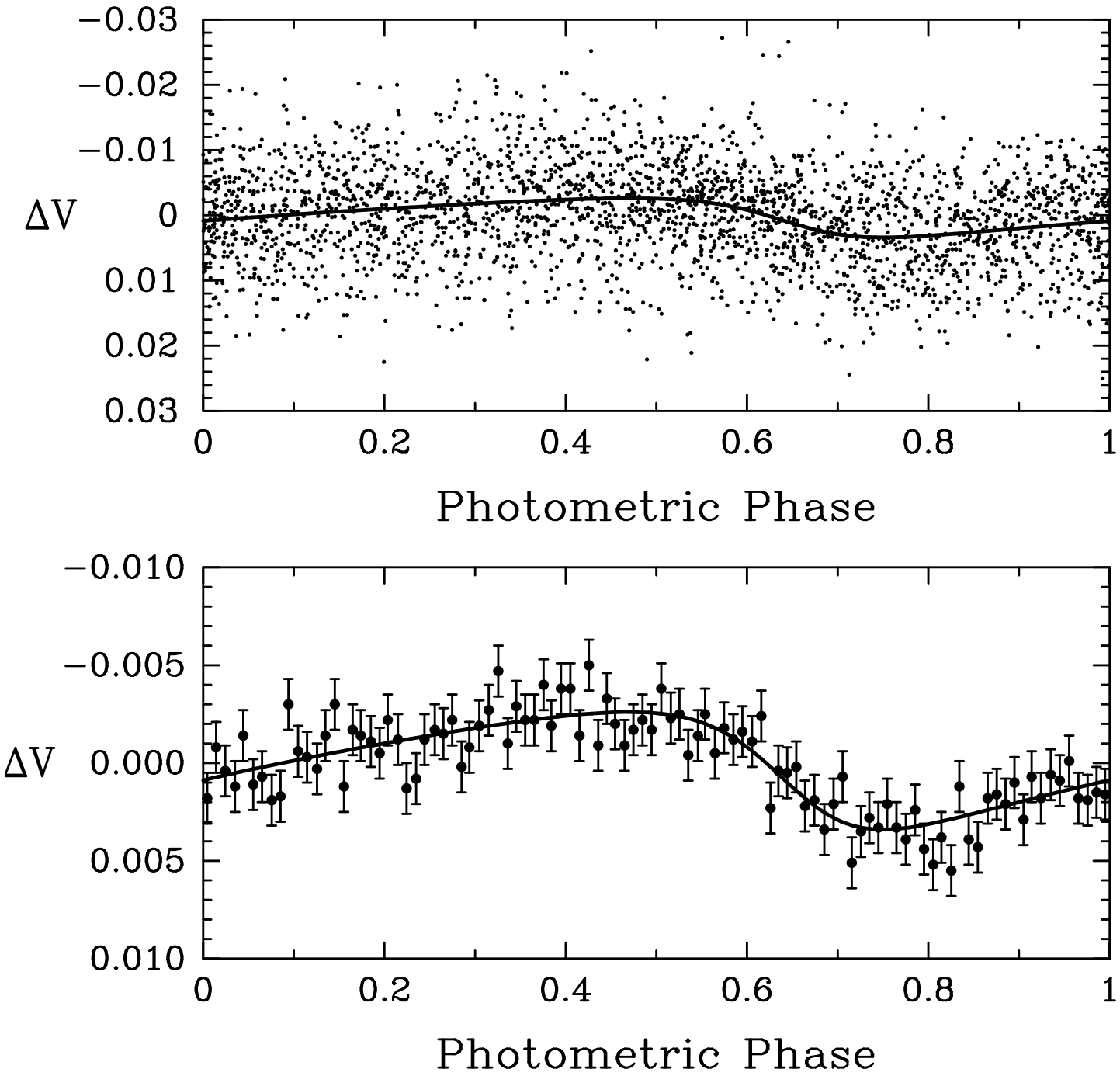
−0.03
−0.02
−0.01
ΔV 0
0.01
0.02
0.03
0
0.2
0.4
0.6
0.8
1
Photometric Phase
−0.010
−0.005
ΔV 0.000
0.005
0.010
0
0.2
0.4
0.6
0.8
1
Photometric Phase